6th ECCOMAS Thematic Conference on the Mechanical Response of Composites
COMPOSITES 2017
J.J.C. Remmers and A. Turon (Editors)

A MIXED-MODE COHESIVE MODEL FOR DELAMINATION WITH ISOTROPIC DAMAGE AND INTERNAL FRICTION

Federica Confalonieri*, Umberto Perego*

*Politecnico di Milano
Piazza Leonardo da Vinci, 32
federica.confalonieri@polimi.it, umberto.perego@polimi.it

Keywords: Mixed-mode delamination, cohesive model

Summary: This work deals with the formulation of a thermodynamically consistent, isotropic damage cohesive model for mixed-mode delamination under variable mode ratio. The proposed model is based on the introduction of an internal friction angle in the tensile case, that allows for an accurate modelling of the interaction between normal and shear openings.

1. INTRODUCTION

Delamination is a common failure mechanism in laminated composite materials, often characterized by mixed-mode loading conditions with variable mode ratio. The capability to accurately predict the progressive mixed-mode delamination in real life engineering applications is a key ingredient in the development of robust design tools. The computational strategies for the numerical simulation of the delamination process are often based on the use of interface elements within the cohesive zone approach (see, for instance, [1, 2, 3]). Among the main difficulties arising in the definition of a robust cohesive model, there are, on the one hand, the necessity to ensure its accuracy and thermodynamic consistency for arbitrary loading paths and, on the other hand, the capability to correctly reproduce the typical growth of fracture energy in passing from Pure Mode I to Pure Mode II. A number of experimental works on composite materials (see e.g. [4] for a comprehensive literature survey) show that the fracture energy in Pure Mode II is typically higher than in Pure Mode I, as a result of a change in the involved micromechanical mechanisms, with a transition from pure mode I loading characterized by matrix cleavage and fiber pull-out, to mode II conditions dominated by the formations of cusps and hackles [5, 6].

A new cohesive model, specifically conceived for mixed mode delamination with variable mode ratio, is presented in this work. The model is based on an isotropic damage formulation and is thermodynamically consistent. The coupling between the normal and the shear behaviour is achieved by projecting the cohesive stress vector onto three unit vectors defining three distinct damage modes, accounting for mixed-mode interaction through a parameter playing the role of an angle of internal friction. The proposed model is able to capture the non-monotonic increase of fracture energy at increasing mode ratios without the need of introducing any empirical law, as demonstrated by the comparison between the outcome of the present cohesive law and the data resulting from experimental tests performed with the Mixed Mode Bending test [7] apparatus.

ISBN: 978-90-386-4366-3

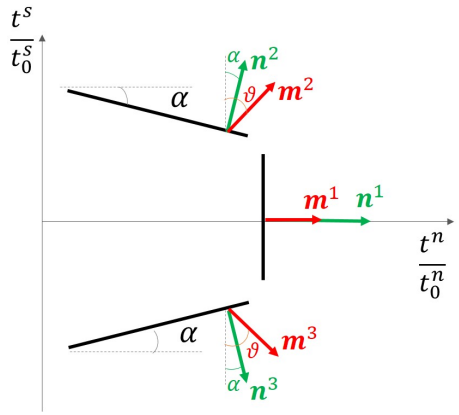

Figure 1. Damage modes

2. FORMULATION

The coupling between the normal and the shear behaviour is achieved by defining the three damage modes, represented in Figure 1, in the plane of non-dimensional cohesive tractions (i.e. the cohesive stresses divided by the corresponding pure Mode peak values). Each damage mode is identified by a unit normal vector $\mathbf{n}^i$ depending on an angle α playing the role of an angle of internal friction.The first damage mode is associated to an opening dominated decohesion process, while the second and third damage modes are the result of the interaction between shear and normal relative displacements. The unit vector $\mathbf{n}^1$ is associated to the opening-dominated mode, while $\mathbf{n}^2$ and $\mathbf{n}^3$ define the two shear-dominated, symmetrical modes.

$$\begin{aligned} \mathbf{n^1} &= [1\ 0] \\ \mathbf{n^2} &= [\sin\alpha\ \ \cos\alpha] \\ \mathbf{n^3} &= [\sin\alpha\ \ -\cos\alpha] \end{aligned} \tag{1}$$

The modelling of the delamination under mixed-mode conditions with variable mode ratios and arbitrary loading paths is obtained formulating an isotropic damage cohesive model in a thermodynamically consistent framework. The free energy per unit surface Ψ is defined as:

$$\Psi = \frac{1}{2} K \left(\langle \delta^n \rangle_-\right)^2 + \frac{1}{2} \left(1-d\right) K \left(\langle \delta^n \rangle_+\right)^2 + \frac{1}{2} \left(1-d\right) K \left(\delta^s\right)^2 \tag{2}$$

being δ^n and δ^s the normal and tangential relative displacements, K the elastic stiffness of the interface and d the isotropic damage variable. The unilateral effect is accounted for by the introduction of the Macauley brackets $\langle\ \rangle$ that allow to distinguish between the tensile and the compressive cases. Within a classical thermodynamic framework, the cohesive tractions t^n and t^s and the strain energy per unit of damage growth Y can be defined by means of the following state equations:

$$t^n = \frac{\partial \Psi}{\partial \delta^n} = K\langle \delta^n \rangle_- + (1-d)\, K\langle \delta^n \rangle_+ \tag{3}$$

$$t^s = \frac{\partial \Psi}{\partial \delta^s} = (1-d)\, K\delta^s = (1-d)\, \frac{t_0^s}{\delta_0^s}\delta^s \tag{4}$$

$$Y = -\frac{\partial \Psi}{\partial d} = \frac{1}{2}K\left(\langle \delta^n \rangle_+\right)^2 + \frac{1}{2}K\left(\delta^s\right)^2 \tag{5}$$

with $t_0^n = K\delta_0^n$ and $t_0^s = K\delta_0^s$, being t_0^n and t_0^s the strengths in pure Modes I and II and δ_0^n and δ_0^s the relative displacements at the onset of delamination, i.e. corresponding to t_0^n and t_0^s. For the sake of simplicity, only the tensile case, i.e. $\delta^n \geq 0$, will be considered in the following.
Let us introduce the vector $\overline{\mathbf{t}}$, collecting the non-dimensional cohesive tractions, i.e:

$$\overline{\mathbf{t}} = \left[\begin{array}{cc} \overline{t}^n & \overline{t}^s \end{array}\right]^T = \left[\begin{array}{cc} \frac{t^n}{t_0^n} & \frac{t^s}{t_0^s} \end{array}\right]^T \tag{6}$$

A vector of effective cohesive stresses $\mathbf{s}$ is introduced to account for the interaction between normal and tangential behaviour: each component $s^i,\ i = 1,2,3$ is computed by projecting $\overline{\mathbf{t}}$ onto the direction defined by one of the three normals in eqn. 1, identifying a distinct damage mode:

$$\begin{aligned} s^1 &= \overline{\mathbf{t}}^T \mathbf{n^1} = \overline{t}^n \\ s^2 &= \overline{\mathbf{t}}^T \mathbf{n^2} = \overline{t}^n \sin\alpha + \overline{t}^s \cos\alpha \\ s^3 &= \overline{\mathbf{t}}^T \mathbf{n^3} = \overline{t}^n \sin\alpha - \overline{t}^s \cos\alpha \end{aligned} \tag{7}$$

In matrix form:

$$\mathbf{s} = \mathbf{N}\overline{\mathbf{t}} \tag{8}$$

where matrix $\mathbf{N} = [\mathbf{n}^1\ \mathbf{n}^2\ \mathbf{n}^3]^T$ gathers the unit vectors $\mathbf{n}^i$. The same approach can be followed also for the relative displacements. Let $\overline{\boldsymbol{\delta}}$ define the vector collecting the non-dimensional opening displacements in the normal and in the tangential directions as:

$$\overline{\boldsymbol{\delta}} = \left[\begin{array}{cc} \overline{\delta}^n & \overline{\delta}^s \end{array}\right]^T = \left[\begin{array}{cc} \frac{\delta^n}{\delta_0^n} & \frac{\delta^s}{\delta_0^s} \end{array}\right]^T \tag{9}$$

A vector $\mathbf{w}$ of effective relative displacements, conjugated to the effective cohesive stresses $\mathbf{s}$ in the expression of the free energy density Ψ, is defined by introducing three structural vectors $\mathbf{m}^i$, defined as:

$$\begin{aligned} \mathbf{m^1} &= a\,[1\ 0]^T \\ \mathbf{m^2} &= b\,[\sin\theta\ \ \cos\theta]^T \\ \mathbf{m^3} &= b\,[\sin\theta\ \ -\cos\theta]^T \end{aligned} \tag{10}$$

As depicted in figure 1, $\mathbf{m^1}$ is aligned to $\mathbf{n^1}$ for symmetry considerations, while the orientation of $\mathbf{m^2}$ and $\mathbf{m^3}$ is defined as a function of the angle θ, different from the angle of internal friction α. The effective relative displacements $w^i,\ i = 1, 2, 3$ are obtained by the the projection of the non-dimensional relative displacements vector $\overline{\boldsymbol{\delta}}$ onto a structural vector $\mathbf{m}^i$ as:

$$\begin{aligned} w^1 &= \overline{\boldsymbol{\delta}}^T \mathbf{m^1} \\ w^2 &= \overline{\boldsymbol{\delta}}^T \mathbf{m^2} \\ w^3 &= \overline{\boldsymbol{\delta}}^T \mathbf{m^3} \end{aligned} \tag{11}$$

In matrix form:

$$\mathbf{w} = \mathbf{M}\overline{\boldsymbol{\delta}} \tag{12}$$

being $\mathbf{M}$ the matrix gathering the components of the three structural vectors $\mathbf{m}^i$.

The strain energy Ψ can be expressed as a function of the effective quantities defined in eqns. 7 and 11 to underline the contribution of each single damage mode.

$$\Psi = \frac{1}{2}\mathbf{t}^T\boldsymbol{\delta} = \underbrace{\frac{1}{2}s^1w^1}_{\Psi^1} + \underbrace{\frac{1}{2}s^2w^2}_{\Psi^2} + \underbrace{\frac{1}{2}s^3w^3}_{\Psi^3} \tag{13}$$

The two unknown constants a and b are, then, determined by imposing that Ψ remains the same in passing from the direct to the effective variables, i.e.

$$\frac{1}{2}\left(t^n\delta^n + t^s\delta^s\right) = \frac{1}{2}\left(s^1w^1 + s^2w^2 + s^3w^3\right) \tag{14}$$

thus, obtaining:

$$a = \left(t_0^n\delta_0^n - t_0^s\delta_0^s\tan\alpha\tan\theta\right) \qquad b = \frac{t_0^s\delta_0^s}{2\cos\alpha\cos\theta} \tag{15}$$

By considering the strain energy Ψ^i associated to each damage mode, the following state equations define three effective strain energies release rates Y^i:

$$\begin{aligned} Y^1 &= -\frac{\partial\Psi^1}{\partial d} = \frac{1}{2}\left(t_0^n\delta_0^n - t_0^s\delta_0^s\tan\alpha\tan\theta\right)\left(\overline{\delta}^n\right)^2 \\ Y^2 &= -\frac{\partial\Psi^2}{\partial d} = \frac{1}{4}t_0^s\delta_0^s\left[\tan\alpha\tan\theta\left(\overline{\delta}^n\right)^2 + \left(\overline{\delta}^s\right)^2 + \left(\tan\alpha + \tan\theta\right)\overline{\delta}^n\overline{\delta}^s\right] \\ Y^3 &= -\frac{\partial\Psi^3}{\partial d} = \frac{1}{4}t_0^s\delta_0^s\left[\tan\alpha\tan\theta\left(\overline{\delta}^n\right)^2 + \left(\overline{\delta}^s\right)^2 - \left(\tan\alpha + \tan\theta\right)\overline{\delta}^n\overline{\delta}^s\right] \end{aligned} \tag{16}$$

that play the role of driving forces acting on the corresponding damage modes, with:

$$Y^1 + Y^2 + Y^3 = \frac{1}{2}t_0^n\delta_0^n\left(\overline{\delta}^n\right)^2 + \frac{1}{2}t_0^s\delta_0^s\left(\overline{\delta}^s\right)^2 = Y \geq 0 \tag{17}$$

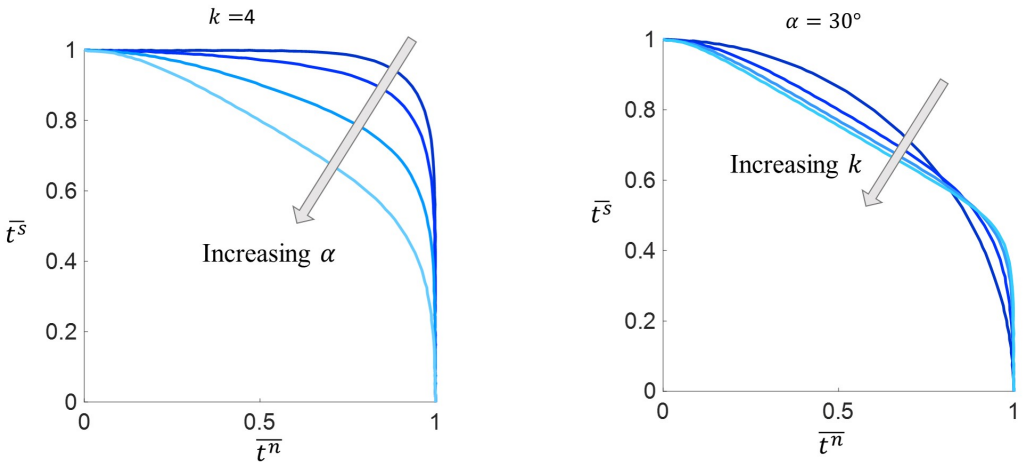

Figure 2. First activation domain: a) for increasing values of α and $k = 4$; b) for increasing values of k and $\alpha = 30°$

In the following, it is assumed that:

$$\theta = \arctan\left(\frac{t_0^n \delta_0^n}{t_0^s \delta_0^s} \tan\alpha\right) \tag{18}$$

so that in the tensile case $Y^1 \geq 0$ for $\alpha < 45°$. On the contrary, either Y^2 or Y^3 can be negative, but their sum $Y^2 + Y^3$, representing the fraction of the strain energy release rate associated to the shear-dominated damage modes, is always non-negative.

The damage activation criterion is written as a function of the strain energy release rates Y^i as:

$$\varphi = \left(\frac{Y^1}{\chi_0^1 + \chi^1}\right)^k + H(Y^2)\left(\frac{Y^2}{\chi_0^2 + \chi^2}\right)^k + H(Y^3)\left(\frac{Y^3}{\chi_0^3 + \chi^3}\right)^k - 1 \leq 0 \tag{19}$$

being the exponent k an input parameter of the model, $H()$ the Heaviside function, introduced to avoid negative contributions of Y^2 and Y^3 to the damage activation function, and $\chi^i + \chi_0^i$ the current threshold for the i-th damage mode, evolving during the decohesion process as a function of the damage variable d. χ_0^i represents the initial threshold, while χ^i is the internal variable, governing the threshold evolution for increasing damage and determines the shape of the softening branch. Figure 2 shows the damage activation surface at the onset of decohesion, for increasing values of the internal friction angle α and $k = 4$ (a) and for increasing values of the exponent k, while maintaining a constant value of the angle $\alpha = 30°$ (b).

In the framework of a classical thermodynamic formulation, the cohesive model is completed by the introduction of the damage evolution law and of the Kuhn-Tucker conditions. The damage rate is obtained by imposing that $\varphi = 0$ and $\dot{\varphi} = 0$, i.e.:

$$\dot{d} = -\frac{\frac{\partial\phi}{\partial\delta^n}\dot{\delta}^n + \frac{\partial\phi}{\partial\delta^s}\dot{\delta}^s}{\frac{\partial\phi}{\partial d}} = \frac{\sum_{i=1}^3 \left(\frac{\partial\phi}{\partial Y^i}\frac{\partial Y^i}{\partial\delta^n}\right)\dot{\delta}^n + \sum_{i=1}^3 \left(\frac{\partial\phi}{\partial Y^i}\frac{\partial Y^i}{\partial\delta^s}\right)\dot{\delta}^s}{\sum_{i=1}^3 \left(\frac{\partial\phi}{\partial\chi^i}\frac{\partial\chi^i}{\partial d}\right)} \tag{20}$$

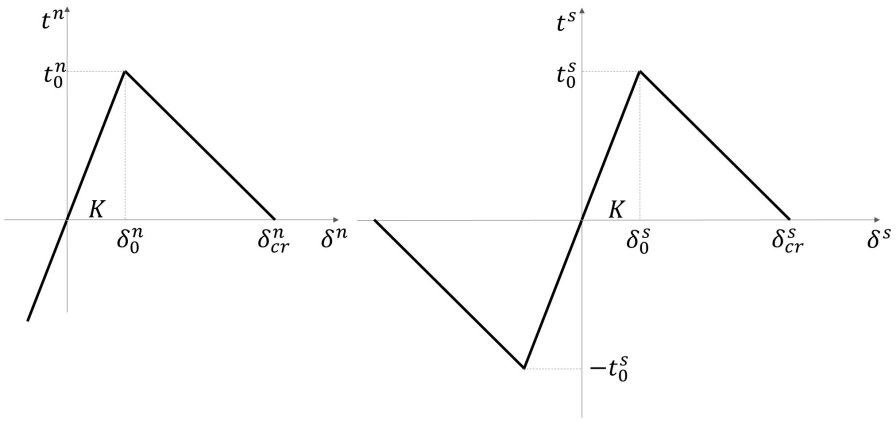

Figure 3. Bilinear traction-separation laws in pure Modes I and II

while the loading-unloading conditions read as:

$$\phi \leq 0 \qquad \dot{d} \geq 0 \qquad \phi \dot{d} = 0 \tag{21}$$

The thermodynamic consistency of the cohesive model can be proven considering the Clausius-Duhem inequality for isothermal processes and showing that the mechanical dissipation is always non negative.

$$D = Y^1 \dot{d} + Y^2 \dot{d} + Y^3 \dot{d} = \left(Y^1 + Y^2 + Y^3\right) \dot{d} = Y \dot{d} \geq 0 \tag{22}$$

The expressions of χ_0^i and χ^i can be found by prescribing a fixed functional form for the two traction-separation laws in pure Modes. In this work, the case of a bilinear shape, shown in Figure 3, is envisaged. Under this hypothesis, the two branches of the pure Mode traction-separation law depicted in Figure 4 can be described as:

$$t = \frac{t_0}{\delta_0} \delta \qquad \text{for} \quad \delta \leq \delta_0 \tag{23}$$

$$t = (1 - d) \frac{t_0}{\delta_0} \delta = t_0 \frac{\delta_{cr} - \delta}{\delta_{cr} - \delta_0} \qquad \text{for} \quad \delta \geq \delta_0 \tag{24}$$

From eqn. 24 it is possible to derive the relation between the damage variable d and the relative displacement δ for $\delta \geq \delta_0$, i.e.

$$\delta = \frac{\delta_{cr} \delta_0}{\delta_{cr} - (\delta_{cr} - \delta_0) d} \tag{25}$$

Pure Mode I and II conditions can be retrieved by imposing that:

$$\delta^n \neq 0 \quad \delta^s = 0 \qquad \text{for pure Mode I} \tag{26}$$

$$\delta^n = 0 \quad \delta^s \neq 0 \qquad \text{for pure Mode II} \tag{27}$$

The effective strain energies per unit of damage growth under pure Mode I and II loading conditions can be found by substituting eqns. 27 into eqn. 16:

$$\begin{aligned} Y^1_{mI} &= \frac{1}{2}\left(t^n_0\delta^n_0 - t^s_0\delta^s_0\tan\alpha\tan\theta\right)\left(\overline{\delta}^n\right)^2 \\ Y^2_{mI} &= \frac{1}{4}t^s_0\delta^s_0\left(\tan\alpha\tan\theta\overline{\delta}^n\right)^s \\ Y^3_{mI} &= \frac{1}{4}t^s_0\delta^s_0\left(\tan\alpha\tan\theta\overline{\delta}^n\right)^s \end{aligned} \tag{28}$$

$$\begin{aligned} Y^1_{mII} &= 0 \\ Y^2_{mII} &= \frac{1}{4}t^s_0\delta^s_0\left(\overline{\delta}^s\right)^s \\ Y^3_{mII} &= \frac{1}{4}t^s_0\delta^s_0\left(\overline{\delta}^s\right)^s \end{aligned} \tag{29}$$

with the subscripts mI and mII denoting pure Mode I and Mode II loading conditions. It could be noticed that the behaviour in pure Mode II is uncoupled since $Y^1_{mII} = 0$, while in pure Mode I one has $Y^2_{mI} \neq 0$ and $Y^3_{mI} \neq 0$. For that reason, it is necessary to deal first with the pure Mode II case and, then, treat the Pure Mode I case on the basis of the results obtained for Mode II.

Because of the symmetry of the two shear dominated damage modes with respect to the axis $t^s = 0$, it turns out that $Y^2_{mII} = Y^3_{mII}$, $\chi^2_0 = \chi^3_0$ and $\chi^2 = \chi^3$. The initial thresholds χ^2_0 and χ^3_0 can be determined by imposing that the activation criterion is fulfilled at the onset of delamination, i.e. $\varphi = 0$ for $d = 0$ and $\overline{\delta}^s = 1$.

$$\varphi = \left(\frac{Y^2_{mII}|_1}{\chi^2_0}\right)^k + \left(\frac{Y^3_{mII}|_1}{\chi^3_0}\right)^k - 1 = 2\left(\frac{Y^2_{mII}|_1}{\chi^2_0}\right)^k - 1 = 0 \quad \rightarrow \quad \chi^2_0 = \chi^3_0 = 2^{\frac{1}{k}}\frac{1}{4}t^s_0\delta^s_0 \tag{30}$$

Similarly, the expressions of χ^2 and χ^3 can be found by imposing that the activation criterion is met for a generic point belonging to the softening branch, i.e that the activation function is zero for $d > 0$ and $\overline{\delta}^s > 1$:

$$\phi = \left(\frac{Y^2_{mII}}{\chi^2_0 + \chi^2}\right)^k + \left(\frac{Y^3_{mII}}{\chi^3_0 + \chi^2}\right)^k - 1 = 0 \quad \rightarrow \quad \chi^2 = \chi^3 = 2^{\frac{1}{k}}\frac{1}{4}t^s_0\delta^s_0\left[\left(\overline{\delta}^s\right)^2 - 1\right] \tag{31}$$

By substituting eqn. 25 into eqn. 31, one obtains:

$$\chi^2 = \chi^3 = 2^{\frac{1}{k}}\frac{1}{4}t^s_0\delta^s_0\left[\frac{\delta^s_{cr}}{\delta^s_{cr} - \left(\delta^s_{cr} - \delta^s_0\right)d}\right]^2 - \chi^2_0 \tag{32}$$

Let us now focus on pure Mode I. The expressions of χ^1_0 and χ^1 can be determined with an analogous procedure, considering the delamination onset and the softening branch, respectively.

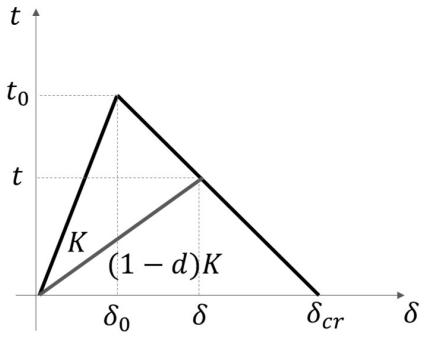

Figure 4. Pure mode bilinear law

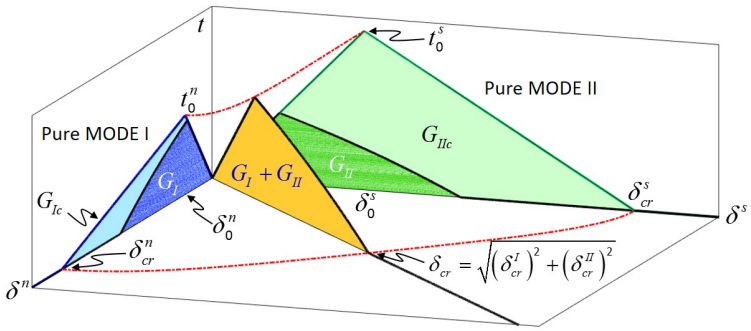

Figure 5. Mixed-mode traction-separation law

For $\overline{\delta}^n = 1$ and $d = 0$, it holds that:

$$\varphi = \left(\frac{Y_{mI}^1|_1}{\chi_0^1}\right)^2 + \left(\frac{Y_{mI}^2|_1}{\chi_0^2}\right)^2 + \left(\frac{Y_{mI}^3|_1}{\chi_0^3}\right)^2 - 1 = 0 \quad \rightarrow \quad \chi_0^1 = \frac{1}{2}\frac{\left(t_0^n\delta_0^n - t_0^s\delta_0^S \tan\alpha \tan\theta\right)}{\left[1 - (\tan\alpha\tan\theta)^2\right]^{\frac{1}{2}}} \tag{33}$$

while for a generic non-dimensional opening displacement $\overline{\delta}^n > 1$ one has:

$$\varphi = \left(\frac{Y_{mI}^1}{\chi_0^1 + \chi^1}\right)^k \left(\frac{Y_{mI}^2}{\chi_0^2 + \chi^2}\right)^k + \left(\frac{Y_{mI}^3}{\chi_0^3 + \chi^2}\right)^k - 1 = 0 \tag{34}$$

and

$$\chi^1 = \frac{\left(t_0^n\delta_0^n - t_0^s\delta_0^S \tan\alpha \tan\theta\right)}{\left\{1 - \left[\left(\frac{\delta_{cr}^n}{\delta_{cr}^s}\frac{\delta_{cr}^s - (\delta_{cr}^s - \delta_0^s)d}{\delta_{cr}^n - (\delta_{cr}^n - \delta_0^n)d}\right)^2 \tan\alpha\tan\theta\right]^k\right\}^{\frac{1}{k}}} \frac{1}{2}\left(\frac{\delta_{cr}^n}{\delta_{cr}^n - (\delta_{cr}^n - \delta_0^n)d}\right)^2 - \chi_0^1 \tag{35}$$

The resulting mixed-mode response is depicted in Figure 5. Even though the pure Modes laws are assumed to be bilinear, the softening branch in the mixed-mode law is, in general,

curvilinear, except that for the particular case of identical pure Modes, i.e. $t_0^n = t_0^s = t_0$, $\delta_0^n = \delta_0^s = \delta_0$ and $\delta_{cr}^n = \delta_{cr}^s = \delta_{cr}$. In this particular case, the resulting mixed-mode traction-separation law can be determined analytically in the case of a radial path, expressing the non-dimensional normal and tangential relative displacements as:

$$\overline{\delta}^n = (1-\beta)\,\overline{\delta} \qquad \overline{\delta}^s = \beta\overline{\delta} \tag{36}$$

By substituting eqns. 36 into enqs. 16 and 19, the activation function turns out to be:

$$\varphi = \left\{ \frac{(1-\beta)^2 \left[1-(\tan\alpha)^{2k}\right]^{\frac{1}{k}} \overline{\delta}^2}{\left[\frac{\delta_{cr}}{\delta_{cr}-(\delta_{cr}-\delta_0)d}\right]^2} \right\}^k + \left\{ \frac{\left[(1-\beta)\tan\alpha+\beta\right]^2 \overline{\delta}^2}{2^{1/k}\left[\frac{\delta_{cr}}{\delta_{cr}-(\delta_{cr}-\delta_0)d}\right]^2} \right\}^k + \\ + \left\{ \frac{\left[(1-\beta)\tan\alpha-\beta\right]^2 \overline{\delta}^2}{2^{1/k}\left[\frac{\delta_{cr}}{\delta_{cr}-(\delta_{cr}-\delta_0)d}\right]^2} \right\}^k - 1 = 0 \tag{37}$$

being $\alpha = \theta$ according to eqn. 18. Solving eqn. 37 for d, the following relationship between the damage variable d and $\overline{\delta}$ holds:

$$d = \frac{\delta_{cr}}{\delta_{cr}-\delta_0}\left(\frac{1}{C_{\beta\alpha}\overline{\delta}}\right) \quad \text{for } \varphi = 0 \qquad \text{with}$$

$$C_{\beta\alpha} = \left\{(1-\beta)^{2k}\left[1-\tan^{2k}\alpha\right] + 0.5\left[(1-\beta)\tan\alpha+\beta\right]^{2k} + 0.5\left[(1-\beta)\tan\alpha-\beta\right]^{2k}\right\}^{\frac{1}{2k}} \tag{38}$$

Thus, from eqns. 3 and 4, for $\varphi = 0$ one obtains:

$$t^n = (1-\beta)\,t_0\left[-C_{\beta\alpha}\delta_0\overline{\delta} + \delta_{cr}\right] \tag{39}$$

$$t^s = \beta t_0\left[-C_{\beta\alpha}\delta_0\overline{\delta} + \delta_{cr}\right] \tag{40}$$

3. NUMERICAL EXAMPLES

One of the strengths of the proposed cohesive model is that the overall fracture energy is an outcome of the interaction between damage modes without the need of introducing any empirical law and without making any assumption on the loading path. In these numerical examples, the effectiveness of the model in capturing the variation of the fracture energy with the mode-mixity ratio is assessed considering the experimental data of three different fiber reinforced composite materials, namely HMF/5322 I[8], IM7/8552 [9] and AS4/PEEK [10], resulting from Mixed Mode Bending tests [7]. The input parameters required for the definition of the proposed cohesive model, i.e. the fracture energies G_{Ic}, G_{IIc} and the peak tractions t_0^n, t_0^s in pure Modes I and II, the internal friction angle α and the exponent k appearing in the activation function ϕ,

Material	G_{Ic} $\frac{mJ}{mm^2}$	G_{IIc} $\frac{mJ}{mm^2}$	t_n^0 MPa	t_s^0 MPa	K $\frac{N}{mm^2}$	α deg	k
HMF/5322	0.3043	0.8039	10	18	10,000	32	10
IM7/8552	0.2085	0.7713	60	90	20,000	36	10
AS4/PEEK	0.969	1.719	75	80	100,000	42.8	1.56

Table 1. Adopted parameters.

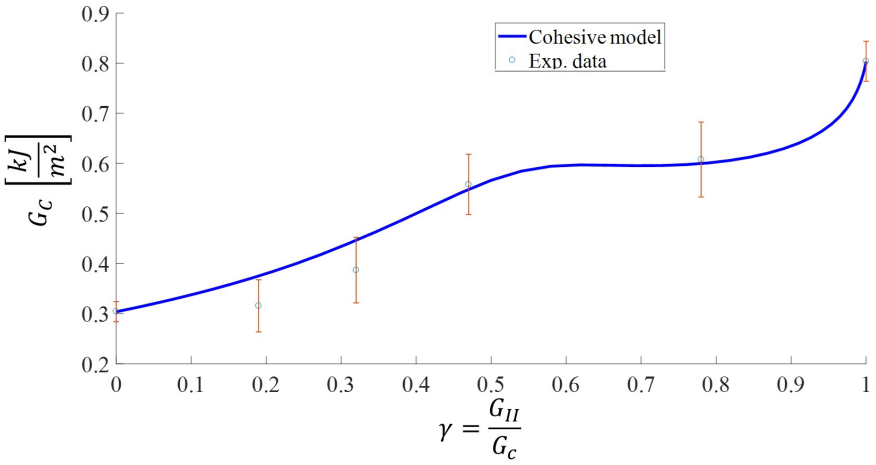

Figure 6. HMF/5322. Experimental vs numerical mixed-mode fracture energies. Dots: experimental data [8]. Solid line: result of the present model.

are listed in Table 1. Figures 6, 7 and 8 show the comparison between the experimental data and the curve obtained with the proposed cohesive law: in all the three cases a good agreement can be observed. In addition, for comparison purposes, the empirical Benzeggagh-Kenane (B-K) law [11] $G_c = G_{Ic} + (G_{IIc} - G_{Ic}) \left(\frac{G_I I}{G_I + G_I I}\right)^{\eta}$ is depicted in Figures 7 and 8, considering the exponent η determined in [9] and [10] by a fitting of the experimental data.

4. CONCLUSIONS

A new isotropic damage cohesive model for the simulation of mixed-mode delamination has been presented in this work. The proposed model is based on the introduction of a dissipation mechanism described by a parameter qualitatively similar to an angle of internal friction, leading in a natural way to a coupling between normal and shear behaviours. The model is thermodynamically consistent and is able to accurately reproduce the fracture energy under mixed-mode loading conditions, as shown in the numerical examples.

5. Acknowledgements

The financial support of Tetra Pak Packaging Solutions is gratefully acknowledged.

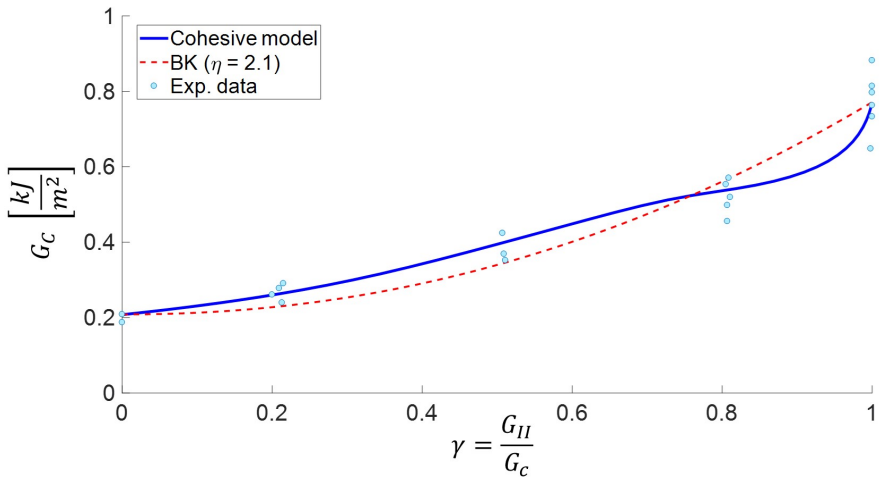

Figure 7. IM7/8552. Experimental vs numerical mixed-mode fracture energies. Dots: experimental data [9]. Dashed line: B-K law [11]. Solid line: result of the present model.

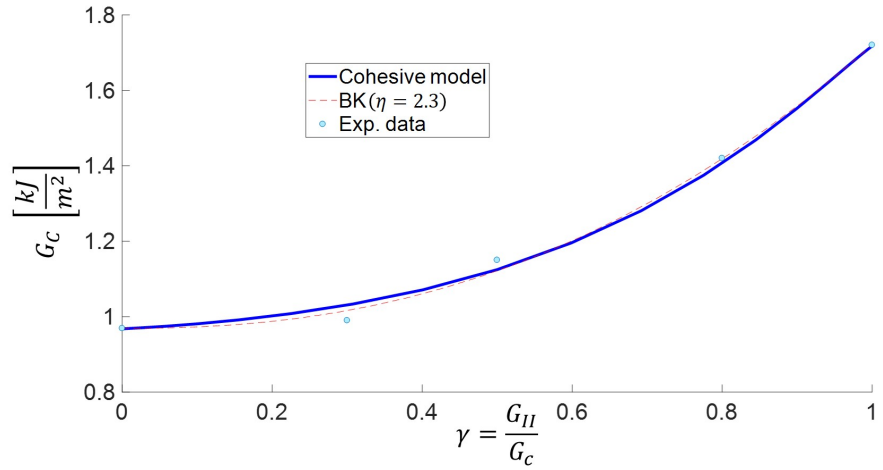

Figure 8. AS4/PEEK. Experimental vs numerical mixed-mode fracture energies. Dots: experimental data [10]. Dashed line: B-K law [11]. Solid line: result of the present model.

References

[1] P.P. Camanho, C.G. Davila, M.F. de Moura, Numerical Simulation of Mixed-mode Progressive Delamination in Composite Materials. *Journal of Composite Materials*, **37**, 1415-1438, 2003.

[2] M.J. Van den Bosch, P.J.G. Schreurs, M.G.D. Geers, An improved description of the exponential Xu and Needleman cohesive zone law for mixed-mode decohesion. *Engineering Fracture Mechanics*, **73**, 1220-1234, 2006.

[3] K. Park, G.H. Paulino, J.R. Roesler, A unified potential-based cohesive model of mixed-mode fracture. *Journal of the Mechanics and Physics of Solids*, **57**, 891-908, 2009.

[4] B.D. Davidson, W. Zhao, An accurate mixed-mode delamination failure criterion for laminated fibrous composites requiring limited experimental input. *Journal of Composite Materials*, **41**, 679-702, 2007.

[5] E.S. Greenalgh, C. Rogers, P. Robinson, Fractographic observations on delamination growth and the subsequent migration through the laminate. *Composites Science and Technology*, **69**, 2345-2351, 2009.

[6] R. Marat-Mendes, M. de Freitas, Fractographic analysis of delamination in glass/fibre epoxy composites. *Journal of Composite Materials*, **47**, 1437-1448, 2013.

[7] J.R. Reeder, J.H. Crews, Mixed-mode bending method for delamination testing. *AIAA Journal*, **28**, 1270-1276, 1990.

[8] N.B. Adeyemi, K.N. Shivakumar, V. S. Avva, Delamination fracture toughness of woven-fabric composites under mixed-mode loading. *AIAA journal*, **37**, 517-520, 1999.

[9] R. Krueger, Development and application of benchmark examples for mixed-mode I/II quasi-static delamination propagation predictions. *NASA report*, 2012.

[10] P. Naghipour, M. Bartsch, L. Chernova, J. Hausmann, H. Voggenreiter, Effect of fiber angle orientation and stacking sequence on mixed mode fracture toughness of carbon fiber reinforced plastics: Numerical and experimental investigations. *Materials Science and Engineering: A*, **527**, 509-517, 2010.

[11] M.L. Benzeggagh, M. Kenane, Measurement of mixed-mode delamination fracture toughness of unidirectional glass/epoxy composites with mixed-mode bending apparatus. *Composites Science and Technology*, **56**, 439–449, 1996.